------ Raf. J. Sci., Vol. 27, No.2, pp. 35-46, 2018------

pEffect of Synthesized Oxiranes and Pyrrolidines on *KMP II* and *LPG 3* genes in *Leishmania infantum* Promastigotes

Haitham L. Al-Hayali
Department of Biology/ College of Science

Abdulwahhab J. Al-Hamadany
Department of Chemistry/ College of Science

Muntaha M. Al-Kattan
Department of Biology/ College of Science
University of Mosul

(Received 24 / 12/ 2017 ; Accepted 21 / 2 / 2018)

ABSTRACT

The research includes synthesis of some heterocycles: oxiranes (O1-O3) through the reaction of chalcones with hydrogen peroxide, and pyrrolidines (P1-P3) by the condensation of chalcones with Schiff bases. The structures of these synthesized heterocycles had been supported by spectral data (1HNMR, IR, UV) and observed their effect on *KMP II* and *LPG 3* genes. The results showed that some compounds gave genetic heterogeneity in these genes suggesting that it could be a good target for treatment of *L. infantum*.

Keywords: *L. infantum*, Oxiranes, Pyrrolidines, *KMP II*, *LPG 3*.

تأثير الأوكسيرانات والبايروليدينات المشيدة على جيني *KMP II* و *LPG 3* في بروماستكوت اللشمانيا الأحشائية *L. infantum*

الملخص

تضمن البحث تشييد عدد من المركبات الحلقية غير المتجانسة وهي الأوكسيرانات (O1−O3) وذلك من خلال تفاعل الجالكونات مع بيروكسيد الهيدروجين كذلك فقد شيدت والبايروليدينات (P1−P3) من تكثيف الجالكونات مع قواعد شف وأن تراكيب هذه الحلقات قد تم دعمها بالبيانات الطيفية (^{1}HNMR و IR وUV) ومن ثم ملاحظة تأثير هذه المركبات على كلٍ من جيني *KMP II* و *LPG3*. أظهرت النتائج أن بعض المركبات أعطت تغايراً وراثياً في هذه الجينات مما يشير إلى إمكانية اعتبار هذين الجينين بوصفهما أهدافاً في معالجة طفيلي اللشمانيا الأحشائية.

الكلمات الدالة: *L. infantum*، الأوكسيرانات، البايروليدينات، *KMP II*، *LPG 3*.

INTRODUCTION

Leishmania parasites are the causative agents of leishmaniasis, one of the World Health Organization's neglected tropical diseases and endemic in 88 countries worldwide. Leishmaniasis was formerly classified as cutaneous, visceral and mucocutaneous forms. However, recently they are categorized into localized, diffuse, chronic cutaneous leishmaniasis, post kala-azar dermal leishmaniasis, visceral leishmaniasis and mucocutaneous leishmaniasis (Azizi *et al.,* 2016).

One of the most serious clinical forms of this disease is visceral leishmaniasis caused by *L. donovani, L. infantum and L. chagasi*, which is invariably fatal if left untreated and over 310 million people are considered at risk of infection (Ruiz-Santaquiteria *et al.,* 2017).

These organisms are digenetic parasites with two basic life cycle stages: one is invertebrate host (Sand fly) and other vertebrate host: Human, Dogs and Rodents (Sachdeva, 2016).

Most of the commonly drugs used of leishmaniasis are toxic, do not cure, failure to treat successfully, and increased the parasite resistance therefore, it is necessary to develop a new medicines that can replace or complement the presently therapeutic available. In recent years, the attentions turn towards the heterocycles are an important class of molecules in organic chemistry, due to their presence in natural products and their use in pharmaceuticals. Heterocycles are the key to biological activity in many small molecule drugs, due to their ability to hydrogen bond and alter polarity at specific sites in the pathogen or host, with the overall effect of inhibiting the biological processes that lead to the progressions of diseases. In addition, heterocycles can impart unique properties to new materials due to their polarity, solubility, and their electronic and optical properties. Furthermore, heterocycles play an important role in biochemical processes because the side groups of the most typical and essential constituents of living cells, DNA and RNA, are based on aromatic heterocycles (Asif, 2017 ; Maruthamuthu *et al.,* 2016).

Kinetoplastid Membrane Protein II (*KMP11*) is a small protein that is highly conserved in all stages of the Leishmania life cycle. This gene is a major constituent of the cell surface of kinetoplastids and is expressed in both promastigote and amastigote. However, the expression of gene is considerably higher in amastigote than that in promastigote, indicating to the relationship of the parasite with the mammalian host (Sannigrahi *et al.,* 2017). In both phases, the protein was found to associate with membrane structures on the cell surface, localizing itself around the flagellar pocket, intracellular vesicles, and flagellum (Sahoo *et al.,* 2009).

Tryptophan's are abundant in *KMP II* protein, prefer to reside near the lipid−water interface and occurrence of mutation leads to trend the tryptophan buried deep inside the protein core or may be decomposed partially or completely resulting in changes of membrane properties (Sannigrahi *et al.,* 2017).

lipophosphoglycan 3 (*LPG 3*) is one of the most important molecules in survival and virulence of Leishmania. It is abundant in membrane surfaces of promastigote, with increased expression occurring during leishmania transformation into metacyclic promastigote. When a host exposed to bitten by infected vector, promastigotes invade the host macrophages through *LPG* molecules and subsequently disrupt different anti-microbial functions of the macrophages including apoptotic, signaling pathways and this can lead to establishment the infection (Hosseini *et al.,* 2016).

LPG3 is one of the *LPG* genes that encodes the Leishmania homolog of the mammalian Endoplasmic Reticulum and it is involved in variety of processes including antigen presentation, folding and assembling of proteins, and secretory pathways. As well, it has immunological properties and it was obtained from Leishmania parasites and uses in the detection of vaccines against it (Pirdel *et al.,* 2012; Razolzadeh *et al.,* 2015 Hosseini *et al.,* 2016).

In the present work, oxiranes and pyrrolidines compounds were synthesized and tested for their antiparasitic activity against *Leishmania infantum* promastigotes by detecting their impact on *KMP11* and *LPG 3* genes.

MATERIALS AND METHODS

Chalcones Synthesis

Chalcones were prepared according to (Vogel, 1989). A mixture of 0.05 mole of sodium hydroxide pellets, (20) ml of water and (12.5) ml of ethanol was magnetically stirred in a (100) ml round-bottomed flask. A 0.043 mole of the substituted acetophenone was poured on the stirred mixture followed by 0.043 mole of benzaldehyde. The temperature of the mixture was kept at (20-25) C° with a vigorous stirring for (2-3) hrs. until the mixture become thick, mixture was then kept in a refrigerator overnight. The product was filtered under vacuum and washed with water until the neutralization of filtrates, then washed with (20) ml of cold ethanol. After drying the crude chalcone in air, it was recrystallized from ethanol. The names, some physical properties data were illustrated in Table (1).

Table 1: Physical properties of substituted chalcones

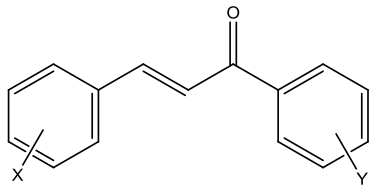

Comp No.	X	Y	Melting point (C°)	Yield (%)	Color
C1	H	4-NO_2	134-136	95	Yellow
C2	4-$N(CH_3)_2$	H	97-99	88	Cumin
C3	3,4-CH_2O_2	H	114-116	64	Earthy
C4	H	4-OCH3	102-104	93	White
C5	3-NO2	H	139-141	99	Pale yellow

Schiff Bases Synthesis

In a 100 ml beaker, (0.01) mole of benzyl amine, (0.01) mole of substituted benzaldehyde and (10) ml of ethanol, after adding was heated for 10 min. at 100 C°. Then the mixture cooled and filtered, the precipitate was dried and recrystallized from ethanol, (Bin *et al.,* 2009). Table (2) illustrates the names and some physical properties.

Table 2: physical properties of substituted schiff bases

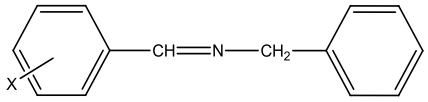

Comp No.	X	Melting point (C°)	Yield (%)	Color
S1	4-NO_2	57-59	54	Crystal yellow-orang
S2	3,4-CH_2O_2	74-76	72	Crystal earthy

Oxiranes Synthesis

5 ml of 30% hydrogen peroxide was added in portion way to a mixture of (0.01) mole of prepared chalcones (C1, C4, C5) in acetone (50) ml and methanol (15) ml containing (1) g NaOH with stirring. The reaction mixture was left overnight, cold water was added and the precipitate was filtered off, washed and crystallized with ethanol (Coffen and Korzan, 1971), as shown in Table (3).

Table 3: physical properties of substituted oxiranes

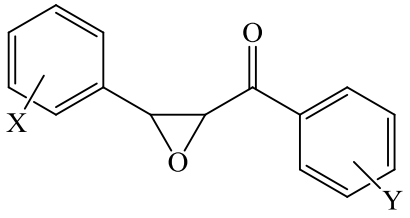

Comp. No.	X	Y	Melting point (C^o)	Yield %	Color
O1	H	4-NO_2	172-175	33	Earthy
O2	H	4-OCH_3	71-73	54	Crystal white
O3	3-NO_2	H	197-200	38	Earthy

Pyrrolidines Synthesis

These compounds were prepared from a mixture of (0.01) mole schiff bases (S1, S2) with (0.01) mole of chalcones (C1, C2, C3). The mixture was magnetically stirred then, (10) ml of ethanol, (3) ml 50% NaOH added and the stirring continues for one hour at room temperature. The mixture was kept overnight, and then add (100) ml of water. The product filtered and washed with water until the neutralization of filtrates, dried and recrystallized by methanol-ethyl acetate (Popandova and Ivanov, 1989), as shown in Table (4).

Table 4: Physical properties of substituted pyrrolidines

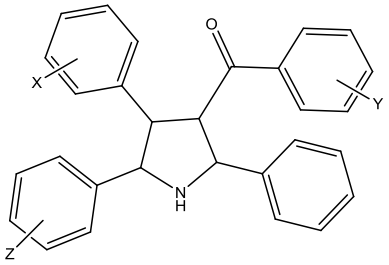

Comp No.	X	Y	Z	Melting point (C°)	Yield (%)	Color
P1	H	4-NO_2	4-NO_2	115-118	53	Pale brown
P2	4-$N(CH_3)_2$	H	3,4-CH_2O_2	65-58	88	Distinct yellow
P3	3,4-CH_2O_2	H	3,4-CH_2O_2	63-65	88	Earthy

DNA Extraction

DNA was extracted according to (Kazemi *et al.*, 2010). Briefly, leishmania promastigotes were grown in tobie`s medium with 15% of blood (Tobie *et al.*, 1950) at 26 C°. Promastigotes were harvested at log phase by centrifugation at 12000 rpm and washed three times with phosphate buffer saline. Washed promastigotes were lysed with lysis buffer (320 mM Glucose, 10 mM Tris base pH 8.5, 5 mM $MgCl_2$, 2% Triton-X 100) at 37 C° for 3 hrs. and boiled for 10 min. Samples were centrifuged at 12000 rpm for 10 min and the supernatant was transferred to a new microfuge tube, were it was subjected to DNA extraction using phenol-chloroform and precipitated with ethanol.

DNA Purity

The concentration, purity of DNA extracted from promastigotes was estimated using Biodrop.

DNA Amplification

The PCR reaction was performed in 20 µl volume containing: 5 µl DNA genomic as a template, 1µl of each primer, 10 µl of master mix and 3 µl of distilled water. Sense and antisense primers were obtained from Genewiz company. The sequence of first gene *KMP II* forward primer: 5' AAGCTTATGGCCACCACGTACGAGGAG 3' and reverse primer: 5' GAATTCTTACTTGGATGGGTACTGCGCAGC 3'. The PCR procedure design included an initial denaturation at 94C° for 2 min, 35 cycles of denaturation at 94C° for 30 sec, annealing at 59C° for 30 sec, extension at 72C° for 30 sec, and then at 7 min. as final extension (Bandani *et al.*, 2014). The sequence of second gene *LPG 3* forward primer: 5' AGATCTATGGCGAACTCGAGCTTGC 3' and reverse primer: 5' GCTAGCCAGATCGTCCTCGCCGACTG 3' The PCR reaction was performed under following condition: 5 min. at 94C° initial denaturation, 35 cycles of 1 min. at 94C° denaturation, 1 min. at 58C° annealing and 2 min. at 72C° extension with 10 min at 72C° final extension (Pirdel, 2016).

The PCR products was separated by electrophoresis on 1.2% agarose gel additive with dye Red Safe DNA (iNtRON) this dye (safe and non-carcinogenic) putting into sodium borate (SB) buffer (Brody and Kern, 2004). The gene bands was visualized under ultraviolet (UV trans-illumonator) and compared with DNA ladder (Biolab).

RESULTS AND DISCUSSION

Chalcones

The substituted chalcones were prepared from benzaldehyde and acetophenone in the presence of NaOH and ethanol as solvent using Claisen-Schmidt condensation. Spectroscopic measurements were used in the diagnosis, UV spectra showed wavelengths at the highest absorption (λ max) for two types of transitions: (n $\longrightarrow$ π*) at range (334-354) nm and (π $\longrightarrow$ π*) a range of (266-324) nm.

On the other hand IR spectra manifested absorption in different locations, the strong range (1649-1662) cm^{-1} referring to stretching vibration of carbonyl group (υ C=O). While the range of the double bond (υ C=C) was (1589-1608) cm^{-1}, and the medium package in range (1502-1574) cm^{-1} related to stretching vibration of aromatic ring bonds (υ C⋯C).

The compound 1-(p-nitro phenyl)-3- phenyl prop-2-ene-l-one **(C1)** showed stretching vibrations, symmetric and asymmetric referred nitro group (υ N⋯O) at (1334) cm^{-1} and (1516) cm^{-1} respectively. Whereas 1-(p-methoxy phenyl)-3-phenyl prop-2-ene-l-one **(C4)** manifested the stretching vibrations, symmetric and asymmetric of ether bond (υ C-O-C) at (1109) cm^{-1} and (1261) cm^{-1} respectively. These values support the synthesized possibility of compounds C1, C4 and others as shown in the Table (5).

Table 5: Spectral data of substituted chalcones C1-C5

Comp. No.	U.V.(λ max)nm $CHCl_3$	IR (KBr disc), υ cm^{-1}			
		C=O	C=C	C⋯C	Others
C1	324 , 354	1662	1591	1574	(N—O) 1516 asym. 1334 sym. ⋯
C2	306 , 336	1649	1597	1529	(C-N) 1167
C3	266 , 334	1658	1589	1502	(C-O-C) 1254 asym. 1107 sym.
C4	278 , 340	1655	1601	1572	(C-O-C) 1261 asym. 1109 sym.
C5	308 , 340	1662	1608	1502	(N—O) 1527 asym. 1350 sym.

The Nuclear Magnetic Resonance ^{1}HNMR has reversed values for chemical shifts of the protons of C1, C2 and C4 as mentioned in the Table (6). We will discuss only NMR spectrum data of chalcone **C4**, the Olefinic protons H2 and H3 showed doublet signal (d) at δ (7.72) and δ (7.96) ppm respectively, whereas the para-substituted ring showed a doublet of doublet (dd) signal for 4H (four protons) at δ (7.10-8.15) ppm and the mono-substituted ring showed a multiplet signal (m) for 5H (five protons) at δ (7.47-7.97) ppm, almost this is evidence lead to correct results. On the other hand, the methoxy (4-OCH3) group revealed a singlet signal (s) for 3H (three protons) at δ (3.85) ppm this results is in agreement with (Mohammed, 2017 ; Rapolu and Srinivasamurthy, 2017 ; Syahri *et al.*, 2016).

Table 6: ^{1}HNMR of substituted chalcones C1, C2 and C4

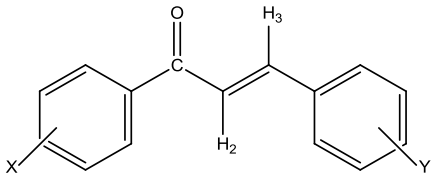

Comp. No.	^{1}H-NMR (DMSO) , δ (ppm)				
	Substituents	Olefinic protons		Aromatic protons	
		H2	H3	Para disubstituted ring	Mono substituted ring
C1	-NO_2	7.75 1H, dd	7.97 1H, dd	7.60-8.40 4H, dd	7.70-8.00 5H, m
C2	-$N(CH_3)_2$ 3.1 6H, s	7.54 1H, dd	7.63 1H, dd	7.70-8.09 4H, dd	7.56-7.70 5H, m
C4	-OCH_3 3.85 3H, s	7.72 1H, d	7.96 1H, d	7.10-8.15 4H, dd	7.47-7.97 5H, m

Schiff Bases

Schiff bases shown in Table (7) prepared by nucleophilic addition of primary amine on aldehyde or ketone carbonyl atom to form carbinol amine which loses H_2O molecule. UV spectra showed wavelengths at the highest absorption (λ max) for two types of transitions: (n ⟶ π*) at range (316-336) nm and (π ⟶ π*) a range of (244-264) nm.

However IR spectra manifested absorption in different locations, the strong range (1637-1641) cm^{-1} referring to stretching vibration of azomethine group (υ C=N), While the medium package in range (1448-1603) cm^{-1} related to stretching vibration of aromatic ring bonds (υ C⋯C) and the range of the single bond (υ C-N) was (1107-1207) cm^{-1}. The compound N-(p-nitrobenzylidene) benzyl amine **(S1)** showed stretching vibrations, symmetric and asymmetric referred nitro group (υ N⋯O) at (1342) cm^{-1} and (1518) cm^{-1} respectively.

Table 7: Spectral data of substituted schiff bases S1 and S2

Comp. No.	U.V.(λ max)nm $CHCl_3$	IR (KBr disc), υ cm^{-1}			
		C=N	C⋯C	C-N	Others
S1	264 , 336	1637	1448	1107	(N—O) 1518 asym. 1342 sym.
S2	244 , 316	1641	1603	1207	(C-O-C) 1255 asym. 1109 sym.

The ^{1}HNMR has reversed values for chemical shifts of the protons of S1 and S2 mentioned in the Table (8). We will discuss only NMR spectrum data of **S1**, the protons $\underline{CH_2}$-N and $\underline{CH}$=N showed singlet signal (s) at δ (4.80) and δ (8.60) ppm respectively, whereas the para-substituted ring showed a doublet of doublet (dd) signal for 4H at δ (8.04-8.31) ppm and the mono-substituted ring showed a multiplet signal (m) for 5H at δ (7.28-7.36) ppm, almost this is evidence lead to correct results. The results which is in agreement with the suggested structures (Dikio *et al.,* 2017 ; Ahmed *et al.,* 2017 ; Patel *et al.,* 2014).

Table 8: ^{1}HNMR of substituted schiff bases S1 and S2

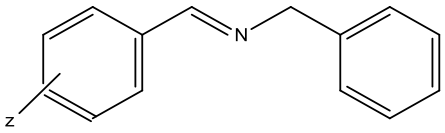

Comp. No.	^{1}H-NMR (DMSO) , δ (ppm)				
	Substituents	CH_2-N	CH=N	Aromatic protons	
				Disubstituted ring	Mono substituted ring
S1	4-NO_2	4.80 2H, s	8.60 1H, s	8.04-8.31 4H, dd	7.28-7.36 5H, m
S2	-OCH_2O 6.10 2H, s	4.70 2H, s	8.40 1H, s	7.00-7.25 3H, m	7.30-7.38 5H, m

Oxiranes

These compounds was produced from the reaction of chalcone with H_2O_2 in basic medium and using ethanol as a solvent. UV spectra showed wavelengths at the highest absorption (λ max) for two types of transitions: (n ⟶ π*) at range (320-338) nm and (π ⟶ π*) a range of (264-308) nm.

As well IR spectra manifested absorption in different locations, the strong range (1664-1685) cm^{-1} related to stretching vibration of carbonyl group (υ C=O), While the medium package in range (1508-1597) cm^{-1} is due to stretching vibration of aromatic ring bonds (υ C⋯C) and the stretching vibrations, symmetric and asymmetric of ether bond (υ C-O-C) at (1072-1109) cm-1 and (1223-1259) cm-1 respectively. The compound 2-(p-nitrobenzoyl)-3-phenyl oxirane **(O1)** showed stretching vibrations, symmetric and asymmetric referred to nitro group (υ N⋯O) at (1346) cm^{-1} and (1518) cm^{-1} respectively. These values support the synthesized possibility of compounds O1 and others as shown in the Table (9).

Table 9: Spectral data of substituted oxiranes O1-O3

Comp. No.	U.V.(λ max)nm $CHCl_3$	IR (KBr disc), υ cm^{-1}			
		C=O	C⋯C	C-O-C	Others
O1	308 , 332	1678	1597	1257 asym. 1109 sym.	(N—O) 1518 asym. 1346 sym.
O2	264 , 320	1664	1508	1259 asym. 1072 sym.	----
O3	304 , 338	1685	1597	1223 asym. 1080 sym.	(N—O) 1529 asym. 1348 sym.

The ^{1}HNMR has reversed values for chemical shifts of the protons of oxiranes as mentioned in the Table (10). We will discuss only ^{1}HNMR spectrum data of **O1**, the Olefinic protons H2 and H3 showed doublet signals (d) at δ (4.75) and δ (4.15) ppm respectively, in addition the para-substituted ring showed a doublet of doublet (dd) signal for 4H at δ (7.92-8.30) ppm and the

mono-substituted ring showed a multiplet signal (m) for 5H at δ (7.00-8.20) ppm, almost this is an evidence lead to correct results. These results are in agreement with suggested structures (Pathipati *et al.*, 2015 ; Thirunarayanan, 2014).

Table 10: ^{1}HNMR of substituted oxiranes O1-O3

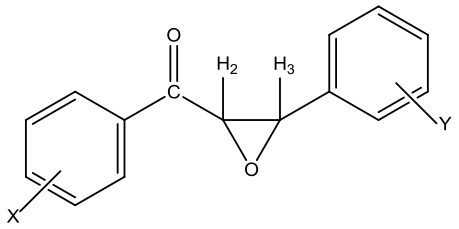

Comp. No.	^{1}H-NMR (DMSO) , δ (ppm)					
	X	Y	Olefinic protons		Aromatic protons	
			H2	H3	Para disubstituted ring	Mono substituted ring
O1	H	4-NO_2	4.75 1H, d	4.15 1H, d	7.92-8.30 4H, dd	7.00-8.20 5H, m
O2	H	4-OCH_3 3.80 3H, s	4.70 1H, d	4.10 1H, d	7.10-8.03 4H, dd	7.39-7.47 5H, m
O3	3-NO_2	H	4.85 1H, d	4.37 1H, d	7.65-8.05 4H, m (meta-disubstituted)	7.05-7.91 5H, m

Pyrrolidines

Finally, schiff bases were condensed with chalcones to give the pyrrolidines. UV spectra showed wavelengths at the highest absorption (λ max) for two types of transitions: (n ⟶ π*) at range (312-340) nm and (π ⟶π*) a range of (256-260) nm.

On the other hand IR spectra manifested absorption in different locations, the strong range (1641-1658) cm^{-1} referring to stretching vibration of carbonyl group (υ C=O), While the medium package in range (1574-1585) cm^{-1} related to stretching vibration of aromatic ring bonds (υ C⋯C), and the range (3437-3454) cm^{-1} related to wide package (NH) bond. The compound 2,4-Diphenyl-3-(p-nitrbenzoyl)-5-(p-nitrophenyl) pyrrolidine **(P1)** showed stretching vibrations, symmetric and asymmetric referred nitro group (υ N⋯O) at (1344) cm^{-1} and (1523) cm^{-1} respectively. These values support the synthesized possibility of compounds P1 and others as shown in the Table (11).

Table 11: Spectral data of substituted pyrrolidine P1-P3

Comp. No.	U.V.(λ max)nm $CHCl_3$	IR (KBr disc), υ cm^{-1}			
		NH	C=O	C⋯C	Others
P1	258 , 338	3442	1641	1585	(N—O) 1523 asym. 1344 sym.
P2	260 , 312	3437	1641	1579	(C-O-C) 1255 asym. 1097 sym.
P3	256 , 340	3454	1658	1574	(C-O-C) 1255 asym. 1105 sym.

The ^{1}HNMR has reversed values for chemical shifts of the protons of pyrrolidines as mentioned in the Table (12). We will discuss only ^{1}HNMR spectrum data of **P1**, the protons H3 and H4 showed triplet signal (t) at δ (4.10) and δ (4.30) ppm respectively, also the H2 and H5 was gave

doublet signal (d) at δ (4.75) and δ (4.95) ppm respectively, as para-substituted ring shown a doublet of doublet (dd) signal for 8H at δ (7.62-8.11) ppm, non-substituted ring showed a multiplet signal (m) for 13H at δ (7.03-8.50) ppm, it is worthy to mention that NH group showed doublet signal (d) at δ (3.15) ppm, almost this is evidence lead to correct results. These results are in agreement with suggested structur (Hassaneen *et al.*, 2017 ; Wagh, 2015 ; Al-Kadhimi *et al.*, 2012).

Table 12: ^{1}HNMR of substituted pyrrolidine P1-P3

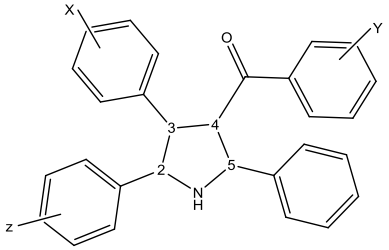

Comp No.	^{1}H-NMR (DMSO) , δ (ppm)									
	X	Y	Z	NH	H3	H4	H2	H5	Aromatic protons	
									Para disubstituted ring	Other Ar-H
P1	H	4-NO_2	4-NO_2	3.15 1H, d	4.10 1H, t	4.30 1H, t	4.75 1H, d	4.95 1H, d	7.62-8.11 8H, dd	7.03-8.50 10H, m
P2	-$N(CH_3)_2$ 3.00 6H, s	H	-OCH_2O- 6.75 2H, d	3.00 1H, d	4.20 1H, t	4.35 1H, t	4.77 1H, d	4.90 1H, d	7.00-8.11 4H, dd	7.24-8.40 13H, m
P3	-OCH_2O- 5.80 2H, s	H	-OCH_2O- 6.12 2H, s	3.10 1H, d	4.15 1H, t	4.37 1H, t	4.70 1H, d	4.89 1H, d	----	7.00-8.40 16H, m (all rings)

Effect of Oxiranes and Pyrrolidines on *KMP II* gene

Fig. (1), showed the size of amplified *KMP II* at 279 bp in control and treated *L. infantum* promastigotes. Some compounds gave a genetic heterogeneity as shown in the size 125 bp in the line 4 refereed to promastigotes treated with O6 compound, line 13 refereed to promastigotes treated with P3 and line 14 refereed to promastigotes treated with P2

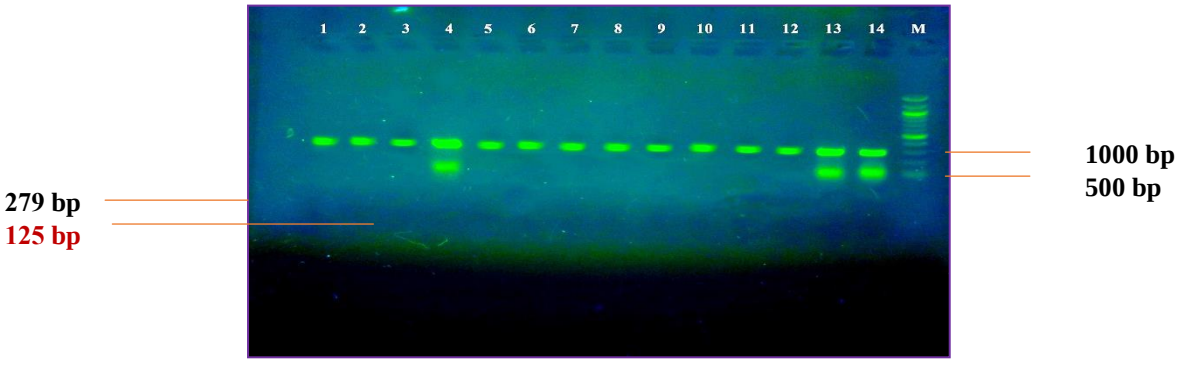

Fig. 1: Electrophoresis of PCR products for *KMP II* of *L. infantum* amplification. M, 100 bp ladder as a marker

The results indicated that the appearance of the hetero packages in treated promastigotes refers to some genetic changes in this gene in comparing with untreated. The bands size of *KMP II* gene is in agreement with (Bandani *et al.*, 2014 ; Soflaei *et al.*, 2012).

(Li and Wang, 2008) they demonstrated that any changes occurred in *KMP II* gene resulted in a dramatic inhibition of cell growth, decreased cell motility, and eventual cell death after 3 days of use RNAi as a silencing in *T. cruzi* parasites. Also suggested that gene depletion did not prevent additional rounds of nuclear division, after 48 hrs. of exposure cells with two nuclei and one kinetoplast increased 25%, cells with multiple nuclei and one kinetoplast increased 30% and those with multiple nuclei and two kinetoplasts increased 18%, this was accompanied by a decrease of natural cells in about 62%.

(Sahoo *et al.*, 2009) mentioned that some of antileishmanial drug, pentamidine was able to find five different binding sites in *KMP II* protein of various *Leishmania* strains and sometimes observed ten different binding conformations, As well reported that vinblastine was reduce mRNA level of this gene in *T. cruzi* and *Leishmania Spp.* as known the vinblastine has no ligand binding site but effect at RNA phase similarly, antimonial compounds and amphotericin B effect on leishmanial *KMP11*. This may be in agreement with our study about the ligand possibility of heterocycles with *KMP II* and affecting on some amino acids.

It is worthy to mentioned (Sannigrahi *et al.*, 2017) found that mutations leads to trend the tryptophan buried deep inside the protein core or may be decomposed resulting in changes of membrane properties. In addition, (Bandani *et al.*, 2014) showed that the mutations in some position of *KMP II* proteins led to a change in structure conformation and stability.

Effect of Oxiranes and Pyrrolidines on *LPG 3* gene:

Fig. (2) showed the size of amplified *LPG 3* at 95 bp in control and treated *L. infantum* promastigotes. Some compounds gave a genetic heterogeneity as shown in the size 300 bp, 250 bp and 140 bp in the line 4 refereed to promastigotes treated with O6 compound and line 13 refereed to promastigotes treated with P3.

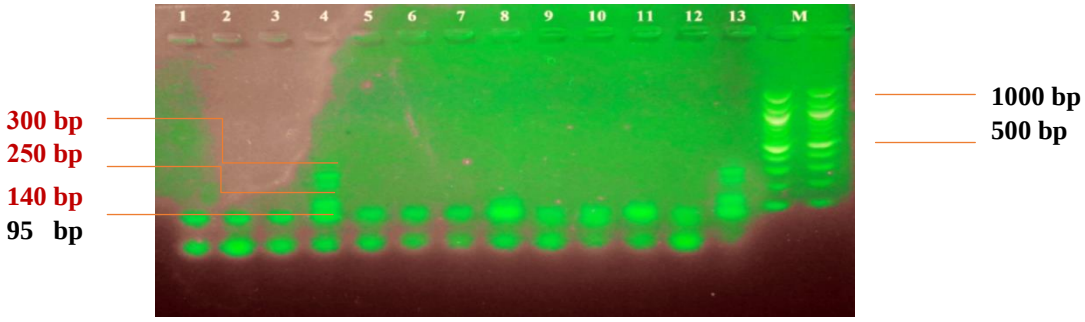

Fig. 2: Electrophoresis of PCR products for *LPG 3* of *L. infantum* amplification. M, 100 bp ladder as a marker

Spath *et al.* (2000) mentioned that *LPG* gene has been implicated in survival of Leishmania in the sand fly gut and stage-regulated binding to the parasite midgut. Also (Naderer and McConville, 2011) demonstrated that Leishmania mutants lacking *LPG* are unable to colonize their sand fly vector, primarily because they cannot bind to the midgut wall of the digestive tract and are rapidly cleared with the remains of the blood meal. As for *L. major* and *L. donovani* mutants lacking *LPG* are poorly virulent in mammalian macrophages and exhibit a characteristic delayed lesion phenotype in susceptible BALB/c mice.

Descoteaux *et al.* (2002) indicated that *LPG 3* mutants show sever defects phosphoglycosylation, resulting in a complete lack of PG assembly on *LPG* and proteins. Finally, Spath *et al.* (2000) showed the *LPG* appear as a surface coat of leishmania parasites additionally, observed in intracellular vesicular structures. Mutants lead to lose this surface in leishmania and intracellular vesicular structures.

In conclusion and from the results monitoring *KMP II* and *LPG 3* may prove to be a feasible target for chemotherapy in *L. infantum*.

REFERENCE

Ahmed, D.S.; El-Hiti, G.A.; Hameed, A.S. (2017). New tetra schiff bases as efficient photostabilizers for poly (vinyl chloride). *Molecules*, **22**, 1506. doi: 10.3390/ molecules 22091506.

Al-Kadhimi, A.A.; AL-Hamdany, A.J.; Jasim, S.S. (2012). Synthesis and antibacterial evaluation of bis-pyrrolidinyl ketones. *RJPBCS*, **3**(1), 908-921.

Asif, M. (2017). A mini review: biological significances of nitrogen heteroatom containing heterocyclic compounds. *Int. J. Bioorg. Chem.*, **2**(3), 146-152.

Azizi, M.H.; Bahadori, M.; Dabiri, S. (2016). A history of leishmaniasis in Iran from 19th century onward. *Arch. Iranian Med.*, **19**(2), 153-162.

Bandani, E.; Soflaei, S.; Khalili, F. (2014). Recombinant plasmid *KMP II* gene of Leishmania major (pc*KMP-11*): production, characterization and sequencing. *Min. Biot*., **26**(3), 175-182.

Bin, L.; Xi-Qun, L.; Wen-Jieomed, Z.; Me-Yun, Z. (2009). Synthesis of ionic liquid supported schiff bases. *ARKIVOC*, **9**, 165-171.

Brody, J.R; Kern, S.E. (2004). Sodium boric acid: a Tris-free, cooler conductive medium for DNA electrophoresis. *BioTech.* **36**(2), 214-216.

Coffen, D.L.; Korzan, D.G. (1971). Synthetic quinine analogs III. Frangomeric and anchimeric processes in the preparation and reactions of α,β-epoxy ketones. *J. Org. Chem.*, **36**(3), 390-395.

Descoteaux, A.; Avila, H.A.; Zhang, K. (2002). Leishmania *LPG 3* encodes a GRP94 homolog required for phosphoiglycan synthesis implicated in parasite virulence but not viability. *EMBO J.*, **21**(17), 4458-4469.

Dikio, C.W.; Okoli, B.J.; Mtunzi, F.M. (2017). Synthesis of new anti-bacterial agents: Hydrazide Schiff bases of vanadium acetylacetonate Complexes. *Cogent Chem.*, **3**, 1336864. doi.org/10.1080/23312009.2017.1336864.

Hassaneen, H.M.E.; Eid, E.M.; Eid, H.A. (2017). Facial regioselective synthesis of novel bioactive spiropyrrolidine/ pyrrolizine-oxindole derivatives via a three components reaction as potential antimicrobial agents. *Molecules*, **22**, 357. doi:10.3390/ molecules 22030357.

Hosseini, M.; Fatahaliha, M.H.; Aghebati-Maleki, H. (2016). Recombinant leishmania major lipophosphoglycan 3 activates human T-lymphocytes via TLR2-independent pathway. *J. Immunotoxicol.*, **13**(2), 263-269.

Kazemi, B.; Tohidi, F.; Bandehpour, M.; Yarian, F. (2010). Molecular cloning, expression and enzymatic assay of pteridine reductase 1 from Iranian lizard leishmania. *Iranian Biomed. J*., **14**(3), 97-102.

Li, Z.; Wang, C.C. (2008). *KMP-11*, a basal body and flagellar protein, is required for cell division in *Trypanosoma brucei*. *Eukary. Cell*, **7**(11), 1941-1950.

Maruthamuthu, S.R.; Stella, C.R.; Bharathi, D.A.G.; Ranjith. R. (2016). The chemistry and biological significance of imidazole, benzimidazole, benzoxazole, tetrazole and quinazolinone nucleus. *J. Chem. Pharm. Res.*, **8**(5), 505-526.

Mohammed, J.H. (2017). Synthesis, characterization, and antibacterial activity of chalcones derivatives. *RJPBCS* **8**(3), 2474-2483.

Naderer, T.; McConville, M.J. (2011). Intracellular growth and pathogenesis of Leishmania parasites. *Essays Biochem.*, **51**, 81-95.

Patel, M.S.; Patel, D.D.; Patel, V.S. (2014). Synthesis of schiff bases of N- based methylene derivatives. *Inter. J. A. Res.*, **2**(3), 580-585.

Pathipati, S.R.; Singh, V.; Eriksson, L.; Selander, N. (2015). Lewis acid catalyzed annulation of nitrones with oxiranes, aziridines, and thiiranes. *Org. Lett.* **17**, 4506-4509.

Pirdel, L. (2016). Comparison of the lipophosphoglycan 3 gene of the lizard and mammalian leishmania: A Homology Modeling. *Res. Mol. Med.,* **4**(2), 15-23.

Pirdel, L.; Hosseini, A.Z.; Kazemi, B. (2012). Cloning and expression of leishmania infantum *LPG3* gene by the lizard leishmania expression system. *Avicenna J. Med. Biotech.,* **4**(4), 186-192.

Popandova-Yambolieva, K.; Ivanov, C. (1989). Synthesis of new spiropyrrolidines and michael addition products using phase transfer catalyzed addition of schiff bases to 9-aryl methylene fluorenes. *Chemica. Scripta.,* **29**, 269-271.

Rapolu, M.; Srinivasamurthy, M. (2017). Biochemical and pharmacological studies of the condensed products of α, β-unsaturated ketones: docking studies. *JPBS,* **12**(4), 14-20.

Rasolzadeh, S.; Fatahaliha, M.H.; Hosseini, M. (2015). Recombinant LPG 3 stimulates IFN-Γ and TNF-A secretion by human NK cells. *Iran J. Parasitol.,* **10**(3), 457-464.

Ruiz-Santaquiteria, M.; Sanchez-Murica, P.A.; Toro, M.A. (2017). First example of peptides targeting the dimer interface of *Leishmania infantum* trypanothione reductase with potent in vitro antileishmanial activity. *Europ. J. Med. Chem.,* **135**(28), 49-59.

Sachdeva, H. (2016). Life cycle of leishmania donovani; causative agent of visceral leishmaniasis: A Review. IJSRSET, **2**(1), 84-85.

Sahoo, G.C.; Rani, M.; Dikhit, M.R. (2009). Structural modeling, evolution and ligand interaction of KMP11 protein of different leishmania strains. *J. Comput. Sci. Syst. Biol.,* **2(2)**, 147-158.

Sannigrahi, A.; Maity, P.; Karmakar, S.; Chattopadhyay, K. (2017). Interaction of *KMP-11* with phospholipid membranes and its implications in leishmaniasis: Effects of single tryptophan mutations and cholesterol. *J. Phys. Chem. B.,* **121**(8), 1824-1834.

Soflaei, S.; Dalimi, A.; Ghafarifar F. (2012). Molecular cloning and expression of the *leishmania infantum KMP-11* gene. *Jundishapur J. Microbiol.,* **6**(2), 132-137.

Spath, G.F.; Epstein, L.; Leader B. (2000). Lipophosphoglycan is a virulence factor distinct from related glycoconjugates in the protozoan parasite *Leishmania major*. *PNAS,* **97**(16), 9258-9263.

Syahri, J.; Purwono, B.; Armunanto, R. (2016). Design of new potential antimalaria compound based on QSAR analysis of chalcone derivatives. *Int. J. Pharm. Sci. Rev. Res.,* **36**(2), 71-76.

Thirunarayanan, G. (2014). Spectral correlation, antimicrobial and insect antifeedant activities of some 1-naphthyl keto-oxiranes. *J. Saudi. Chem. Soc.,* **18**, 854-863.

Tobie, E.J.; Brand, T.V.; Mehlman, B. (1950). Cultural and physiological observations on *Trypanosoma rhodesiense* and *Trypanosoma gambiense*. *J. Parasitol.,* **36**, 48-54.

Vogel, A. (1989). "Practical Organic Chemistry". Longmans, 5th ed. P.1034.

Wagh, S.P. (2015). Synthesis of 3,4-Diylidine and N-substituted pyrrolidines and its anti-microbial activity. *Am. J. Pharm. Tech. Res.,* **5**(3), 153-159.